

Highlighting research results from the lab led by Prof. José E. Báez in the Department of Chemistry at the University of Guanajuato (UG), Guanajuato, Gto. México, in collaboration with Prof. Moustapha Bah at the Autonomous University of Querétaro (UAQ), Querétaro, Qro. México.

Synthesis and characterization of segmented poly(ester-urethane)s (PEUs) containing carotenoids

Eloy Rodríguez-deLeón, José E. Báez, and coworkers worked with three different carotenoids such as lutein, zeaxanthin, and astaxanthin, which were used as chain-extender agents in the synthesis of a new family of segmented poly(ester-urethane)s (PEUs) films derived from poly( $\epsilon$ -caprolactone) (PCL) and 1,6-hexamethylene diisocyanate (HDI). The characterization demonstrated the incorporation of the carotenoids in the main chain of the PEUs, and a plastic behavior was observed for the PEUs films.

### As featured in:



See Moustapha Bah, José E. Báez et al., *Polym. Chem.*, 2019, **10**, 6580.



Cite this: *Polym. Chem.*, 2019, **10**, 6580–6587  
 DOI: 10.1039/c9py01487j

Received 3rd October 2019,  
 Accepted 22nd November 2019

rsc.li/polymers

## Introduction

Carotenoids are a group of compounds that play key roles in nature, especially in plants and some microorganisms, because these molecules are part of the photosynthetic machinery regulating the flow of energy and protecting the photosynthetic system against possible damage induced by light.<sup>1,2</sup> Currently, there are more than 750 known carotenoids distributed throughout nature.<sup>3,4</sup> The family of carotenoids is divided into two classes: carotenes (tetraterpenes comprising only carbon and hydrogen) and xanthophylls (oxygen-containing carotenes).<sup>5,6</sup> Lutein (**1**) and zeaxanthin (**2**) (Fig. 1) are yellow-colored xanthophylls that are selectively accumulated in the human retina, specifically in the zone known as macula lutea.<sup>7</sup> Compounds **1** and **2** are key factors protecting against the visual loss associated with the age-related macular degeneration (AMD).<sup>8,9</sup> Due to the low hydrophilicity of xanthophylls, a number of different publications have reported

<sup>a</sup>Posgrado en Ciencias Químico Biológicas, Faculty of Chemistry, Autonomous University of Querétaro (UAQ), Cerro de Las Campanas, Querétaro, Qro. 76010 Mexico. E-mail: moubah@uag.mx

<sup>b</sup>Department of Chemistry, Division of Natural and Exact Sciences (DCNE), University of Guanajuato (UG), Campus Guanajuato, Noria Alta S/N, Guanajuato, Gto. 36050 Mexico. E-mail: jebaez@ugto.mx

<sup>c</sup>Centro de Investigación en Materiales Avanzados S.C. (CIMAV-Unidad Monterrey), Av. Alianza Norte 202, PIIT, Autopista Monterrey-Aeropuerto Km 10, Apodaca, N.L., 66628 Mexico

<sup>d</sup>Centro Física Aplicada y Tecnología Avanzada (CFATA) de la Universidad Nacional Autónoma de México (UNAM), Boulevard Juriquilla 3001, Querétaro, Qro. 76230 Mexico

† Electronic supplementary information (ESI) available. See DOI: 10.1039/c9py01487j

the synthesis of lutein-derived compounds that represent water soluble (or at least water-dispersible) xanthophylls, providing increased bioavailability. In addition, a number of hydrophilic molecules derived from the red xanthophyll astaxanthin (**3**) have been synthesized. Maybe the most famous of these derivatives is the formerly available drug Cardax, a disuccinic sodium salt of **3** aimed to attenuate myocardial damage.<sup>10–12</sup> From another perspective, the development of biodegradable polymers as new ecofriendly materials,<sup>13,14</sup> and the current need to incorporate bioactive molecules into polymeric systems for *in vivo* delivery applications, has been an area of high interest in recent years.<sup>15</sup> Examples of bioactive compounds in polymeric systems are the curcumin biodegradable polymers, which show good cytotoxic effects towards a range of cancer cell lines.<sup>16,17</sup> However, molecules with important biological activities such as carotenoids could be useful to create the new example of so-called “polyactives”.<sup>18</sup> Of the carotenoid-derived polymers published to date, there are only two papers in which astaxanthin was used, although the stereochemistry of the isomer employed in

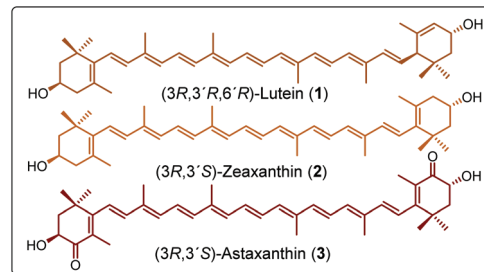


Fig. 1 Structure of carotenoids used in this work.



these reports is unknown. In the first report, astaxanthin was used as a bifunctional initiator in the ring-opening polymerization (ROP) synthesis of polylactides.<sup>15</sup> In the second contribution, it was used as co-monomer to prepare bioactive polymers using different dicarboxylic acids; these compounds were targeted in order to develop new materials with antimicrobial properties for *in vivo* applications.<sup>18</sup> Since xanthophylls such as **1**, **2**, and **3** are diols (Fig. 1), they can be good initiators for the production of polyesters such as poly( $\epsilon$ -caprolactone)s.<sup>19</sup>

In addition, carotenoids have never been used as chain extender agents in the synthesis of poly(ester-urethane)s (PEUs). In this work, we have used three natural xanthophylls, compounds **1**, **2**, and **3**, making the first successful use of xanthophylls as chain-extender agents to prepare segmented polyurethane films. The next two points justify this work: (a) the monomers (carotenoids) are from renewable resources and used in the preparation of a new family of segmented PEUs and (b) the comparison of PEUs derived from carotenoids with respect to PEUs derived from a conventional aliphatic diol. Additionally, the use of natural-based products (such as carotenoids) as building blocks as alternatives to petroleum-based resources is one important step towards more sustainable materials. These PEUs are new smart polymers, which could potentially possess antioxidants and photo-protector abilities.

## Experimental section

### Materials

All reagents,  $\epsilon$ -caprolactone (CL), 1,6-hexamethylene diisocyanate (HDI), 1,8-octanediol (Oct), tin(II) 2-ethylhexanoate [ $\text{Sn}(\text{Oct})_2$ ], and the solvents 1,2-dichloroethane (DCE) and deuterated chloroform ( $\text{CDCl}_3$ ) were purchased from Sigma Aldrich Co. (St Louis, MO, USA) and used as received. Size-exclusion chromatography (SEC) solvents were purchased from Baker-Mallinckrodt (JT Baker, Mallinckrodt Baker Inc., Phillipsburg, NJ, USA). (*3R,3'R,6'R*)-Lutein (**1**) was extracted from a Mexican marigold oleoresin (*Tagetes erecta* L.), while (*3R,3'S*)-zeaxanthin (**2**) was obtained through a base-catalyzed isomerization reaction of **1**. Compound **2** was further oxidized to produce (*3R,3'S*)-astaxanthin (**3**) (as we have described previously<sup>20</sup>). Usually, xanthophylls are very expensive chemical compounds,<sup>21</sup> and this is the reason for only a couple of reports in polymer chemistry that has been previously published.<sup>15,18</sup>

### Instruments

FT-IR spectra of the all xanthophylls, macrodiols, and PEUs films were recorded on a PerkinElmer Spectrum 100 FT-IR spectrophotometer with attenuated total reflectance spectroscopy (ATR) accessory.  $^1\text{H}$  and  $^{13}\text{C}$  NMR spectra were recorded at room temperature on a 500 MHz Bruker Avance III HD instrument, using  $\text{CDCl}_3$  as solvent. Chemical Shifts are reported as  $\delta$  in parts per million (ppm) and referenced to the chemical shift of the residual solvent ( $^{13}\text{C}$  at  $\delta$  77.16, and  $^1\text{H}$  at  $\delta$  7.26, for  $\text{CDCl}_3$ ). SEC was used to determine the number-

average molecular weight ( $M_n$ ) and dispersity ( $D_M$ ) of the synthesized macrodiols with a SEC 1260 Infinity Agilent Technologies. THF was the mobile phase at a flow rate of 1.0  $\text{mL min}^{-1}$  at 37 °C using a column PLgel 5  $\mu\text{m}$  MIXED-D and coupled to a refractive index detector 1260 RID. The results are reported relative to polystyrene standards. The measurements of the matrix-assisted laser desorption and ionization of time of flight (MALDI-TOF) were recorded in the reflectron mode by using an AB SCIEX TOF/TOF 5800 SYSTEM equipped with a nitrogen laser emitting at 349 nm, an input bandwidth = 1000 MHz with a 3 ns pulse width, and working in positive mode. 2,5-Dihydroxybenzoic acid (DHB) was used as matrix in a concentration of 10 mg  $\text{mL}^{-1}$  in THF as a solvent. Polymer samples (3 mg  $\text{mL}^{-1}$ ) were dissolved in THF at room temperature, and then 10  $\mu\text{L}$  of sample solution was mixed with 10  $\mu\text{L}$  of matrix solution (50/50, vol/vol) and mixed in vortex. Different aliquots were placed on a stainless-steel plate, and the solvent was evaporated to make the film before start the acquisition. Thermograms were performed in a Differential Scanning Calorimetry (DSC) Q200 instrument. Three scans were obtained with two heating (0–100 °C, 100 to –30 °C, and –30 to 100 °C). The rate of heating/cooling was 10 °C  $\text{min}^{-1}$  under a nitrogen purge. The melting points ( $T_m$ ) are given as the minimum of the endothermic transition, and the data presented are taken from the second heating scan. Tensile measurements were performed with a Zwick/Roell model Z005 equipped with a 500 N load cell. The tensile test was performed at a test speed of 200  $\text{mm min}^{-1}$ .

### Synthesis of poly( $\epsilon$ -caprolactone) macrodiols (HOPCLOH)

Polymerization was performed in a previously dried 25 ml round-bottom flask.  $\epsilon$ -Caprolactone (CL) (50 mmol, 5.707 g), ammonium heptamolybdate tetrahydrate ( $(\text{NH}_4)_6[\text{Mo}_7\text{O}_{24}] \cdot 4\text{H}_2\text{O}$ ) (Hep,  $2.42 \times 10^{-3}$  mmol, 3 mg), and 1,8-octanediol (Oct) (5 mmol, 590 mg) (CL/Oct = 10) were charged and heated to reflux by stirring them in an oil bath at 150 °C for 1 hour. Ammonium decamolybdate ( $(\text{NH}_4)_8[\text{Mo}_{10}\text{O}_{34}]$ ) was obtained *in situ* in solid state by thermal decomposition of ammonium heptamolybdate.<sup>22–24</sup> The macrodiols obtained and analysed were used without purification. Number-average molecular weight ( $M_n$ ) and conversion were monitored by  $^1\text{H}$  NMR (Fig. S1–S4†).  $M_n(\text{theo}) = 1280$ ,  $M_n(\text{NMR}) = 1200$ ,  $M_n(\text{SEC}) = 2220$ ,  $D_M = 1.36$  (Conv. = 99%). IR ( $\text{cm}^{-1}$ ) 3440 ( $\nu$ , OH), 2934 ( $\nu_{\text{as}}$ , CH<sub>2</sub>), 2861 ( $\nu_s$ , CH<sub>2</sub>), 1722 ( $\nu$ , C=O), 1162 ( $\nu$ , C–(C=O)–O), 732 ( $\rho$ , CH<sub>2</sub>). NMR data for HOPCLOH.  $^1\text{H}$  NMR (500 MHz,  $\text{CDCl}_3$ , ppm):  $\delta$  4.06 (t, 2H, [CH<sub>2</sub>O], PCL and Oct), 3.65 (t, 4H,  $[(\text{CH}_2\text{OH})_2]$ , PCL and Oct), 2.31 (t, 2H, (CH<sub>2</sub>–CO–O), CL), 1.64 (m, 4H,  $[(\text{CH}_2)_2]$ , PCL), 1.59 (q, 4H,  $[(\text{CH}_2)_2]$ , Oct), 1.40 (q, 2H, [CH<sub>2</sub>], CL), 1.33 (8H,  $[(\text{CH}_2)_4]$ , Oct).

### Synthesis of poly(ester-urethane)s (PEUs) derived from poly( $\epsilon$ -caprolactone) diol (HOPCLOH), 1,6-hexamethylene diisocyanate (HDI), and carotenoids **1**, **2**, and **3** as chain extenders

Synthesis of sixteen PEUs were carried out in a 25 mL round-bottom flask previously dried by using the prepolymer method (2 steps) [PEU: Oct(20), 1(20), 2(20), 3(20), Oct(15), 1(15), 2(15),



3(15), Oct(10), 1(10), 2(10), 3(10), Oct(5), 1(5), 2(5), and 3(5)]. An example of this process is briefly described here: first step (prepolymer)- $\alpha,\omega$ -telechelic poly( $\epsilon$ -caprolactone) diol (HOPCLOH,  $M_n$ (NMR) = 1200) (1.058 g, 0.882 mmol), 1,6-hexamethylene diisocyanate (HDI) (232 mg, 1.368 mmol), tin(II) 2-ethylhexanoate (24 mg, two drops) as catalyst, and 8 mL of 1,2-dichloroethane (DCE) as solvent. The reaction mixture was heated in a reflux system with stirring at 80 °C for 1 hour. The second step (addition of chain extender) after prepolymerization, compound 3 (256 mg, 0.441 mmol) was added, and the mixture was stirred for a further 30 minutes at 80 °C. In addition, four PEUs: Oct(10)<sup>b</sup>, 1(10)<sup>b</sup>, 2(10)<sup>b</sup>, and 3(10)<sup>b</sup> (Table 2) were synthesized in a one-pot route.

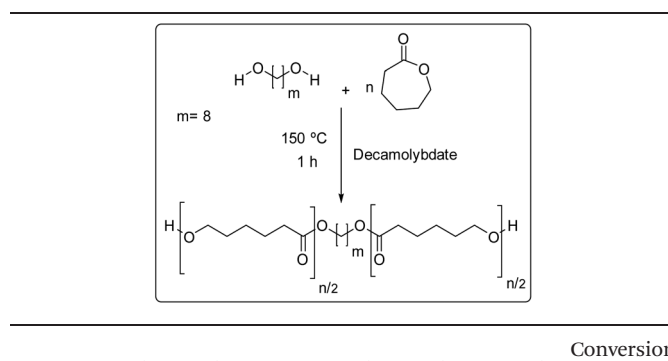
### Synthesis of poly(urethane-carotenoid) (hard segment)

These reactions were carried out in a 25 mL round-bottom flask previously dried. In a reaction example, xanthophyll 1 (0.5 mmol), 1,6-hexamethylene diisocyanate (HDI) (0.55 mmol), tin(II) 2-ethylhexanoate (12 mg, one drop) as catalyst, and 4 mL of 1,2-dichloroethane (DCE) as solvent were loaded and heated in a reflux system with stirring at 80 °C. The time of reaction was 3 hours and then the solvent was slowly evaporated in the fume hood. The material obtained was analyzed without purification.

## Results and discussion

For the synthesis of the PEUs, four different macrodiols (HOPCLOH) derived from 1,8-octanediol (Oct) and CL, with degrees of polymerization (DP) equal to 5, 10, 15, and 20, were obtained by ROP using decamolybdate  $[(\text{NH}_4)_8\text{Mo}_{10}\text{O}_{34}]$  as catalyst.<sup>22–24</sup> The macrodiols were successfully obtained with excellent conversions (from 97 to 99%). The experimental

**Table 1** Macrodiools (HOPCLOH) synthesis from 1,8-octanediol (Oct) and CL



$[\text{CL}]/[\text{I}]^a$	DP <sup>b</sup>	$M_n$ <sup>b</sup>	$M_n$ <sup>c</sup>	$M_n$ <sup>d</sup>	$D_M$ <sup>d,e</sup>	Ratio <sup>f</sup>	Conversion (%)
5	5.0	645	716	1240	1.36	0.52	99
10	9.9	1200	1280	2220	1.36	0.54	99
15	15.0	1670	1850	3680	1.35	0.45	99
20	19.4	2190	2420	6610	1.35	0.33	97

<sup>a</sup> [CL]/[initiator]. <sup>b</sup> Determined by  $^1\text{H}$  NMR in  $\text{CDCl}_3$ . <sup>c</sup> Theoretical value. <sup>d</sup> Determined by size-exclusion chromatography (SEC) analysis. <sup>e</sup>  $D_M$ : dispersity. <sup>f</sup>  $M_n$ (NMR)/ $M_n$ (SEC) ratio.

number-average molecular weight ( $M_n$ ) values for these macrodiols (obtained by SEC) were between 1200 and 6600 g mol<sup>-1</sup> (Table 1). NMR spectra of the macrodiols corroborated the terminal groups (Fig. S1–S4<sup>†</sup>).

Experimental values of  $M_n$  calculated from SEC are higher than  $M_n$  derived from NMR end-group analysis. Overestimation of  $M_n$  obtained by SEC for PCL is a common feature. The  $M_n$ (NMR)/ $M_n$ (SEC) ratio exhibited values between 0.33 and 0.54 (Table 1, penultimate column). In previous contributions these values are similar.<sup>22–24</sup> This effect is attributed to the differences in the hydrodynamic radius between polystyrene standards and the PCL samples.

The MALDI-TOF mass spectrum for  $\alpha,\omega$ -telechelic poly( $\epsilon$ -caprolactone) diol (HOPCLOH) [ $M_n$ (NMR) = 645] is shown in

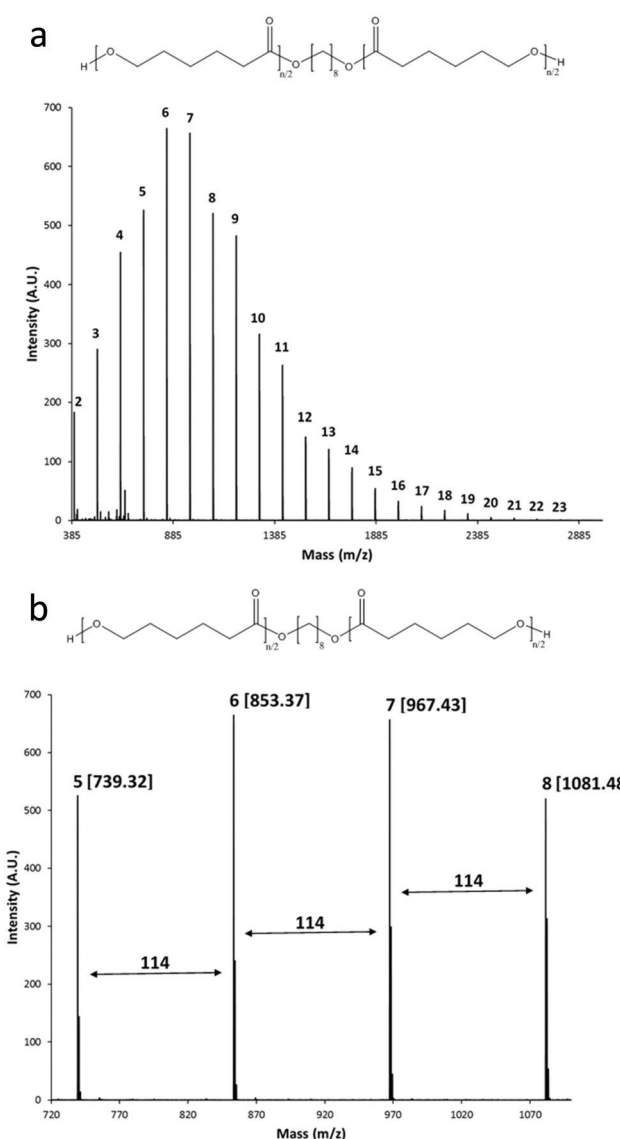


**Fig. 2** (a) MALDI TOF mass spectrum of the HOPCLOH ( $M_n$ (NMR) = 645, Table 1, first line), the number indicates the degree of polymerization (DP) of each peak, and (b) expanded view for the 5–8 CL repeating units, in brackets the mass with sodium doped, 114 is the molecular weight of the CL monomer.

Fig. 2. The curve profile indicates a unimodal distribution (Fig. 2a), similar to that observed in the SEC chromatogram. In Fig. 2b, an expansion view illustrates the oligomers with 5–8 CL repeating units. All peaks are doped with sodium, and the mass is according to the chemical structure of the PCL macrodiol (HOPCLOH). Additionally, incorporation of the hydroxyl terminal groups was detected by NMR spectrum. Signals for macrocyclic species ( $CL_n$ ) are not observed, which indicates that intramolecular transesterification reactions do not occur under these conditions. In Fig. 3, for the peak with  $DP = 5$ , a comparison between the experimental and simulated spectrum is illustrated, where both spectra showed a good agreement.

Later, the macrodiols (HOPCLOH) (with  $DP = 5, 10, 15$  or  $20$ ) were reacted with HDI with a molar ratio  $1:1.55$  in the presence of tin(II) octoate [ $Sn(Oct)_2$ ] as catalyst and 1,2-dichloroethane (DCE) as a solvent, for 1 hour at  $80\text{ }^\circ\text{C}$  to obtain a prepolymer. After this time, the chain extender ( $0.5\text{ mmol}$  of carotenoid **1**, **2** or **3**) was added (Scheme 1). The reaction was stirred for a period of time between 1.3 and 5 hours, and the reaction was stopped when the solution became viscous. Once

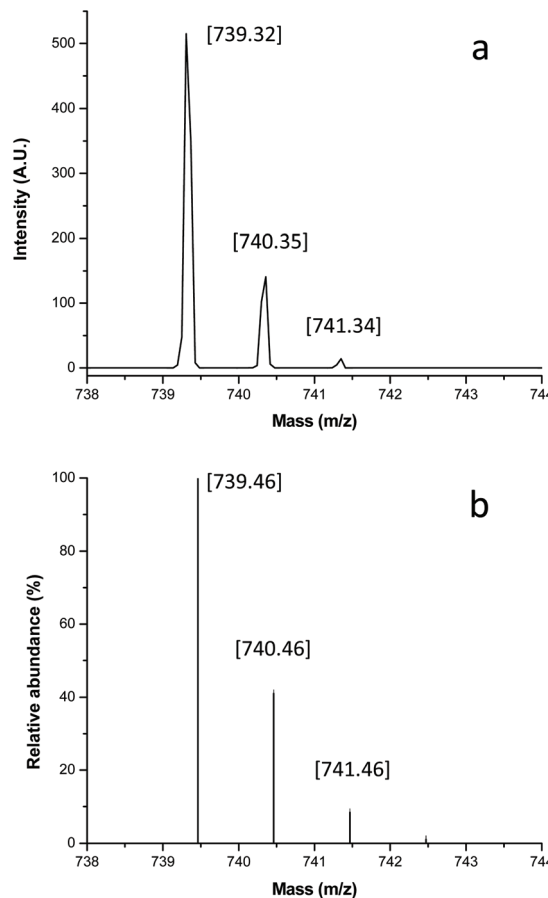
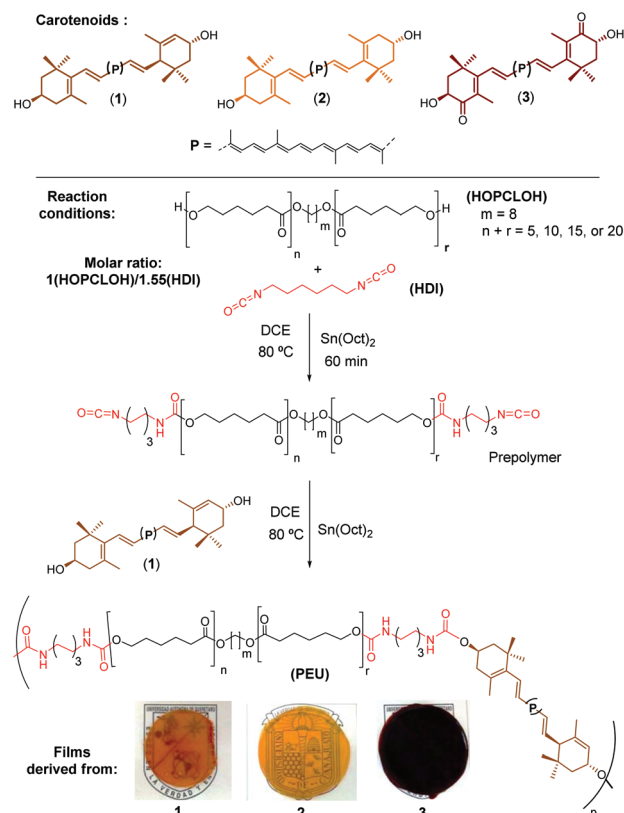


Fig. 3 MALDI-TOF mass spectrum view for the  $738\text{--}744\text{ }m/z$  fragments of the HOPCLOH (Fig. 2b), degree of polymerization (DP) = 5 [ $OctPCL_5, HO(CH_2)_8O[CO(CH_2)_5O]_5H Na^+$ ]. (a) experimental spectrum, and (b) isotopic distribution calculated for DP = 5 [ $C_{38}O_{12}H_{68}Na^+$ , in <http://www.chemcalc.org>].<sup>25</sup> The mass with doped sodium is given in brackets.



Scheme 1 Synthesis of PEUs using **1**, **2**, and **3** as chain extenders (Table 2).

the reaction was finished, the solvent was slowly evaporated by casting into a glass mold with a PTFE surface at the bottom of the fume hood to form the respective films (Scheme 1).

For comparison, five PEUs were synthesized using Oct as chain extender and the same prepolymer derived from macrodiols with DPs of 5, 10, 15 or 20. Some PEU films were characterized using  $^1\text{H}$  and  $^{13}\text{C}$  NMR spectra, while others could not be characterized, due to their very low solubility, even in hot DMSO.

Fig. 4 shows the  $^{13}\text{C}$  NMR spectra of compound **2** (Fig. 4a) and the PEU obtained from **2** and a macrodiol with  $DP = 20$  (Fig. 4b). The assignment of different signals of the NMR spectrum was using 2D NMR spectra (ESI $\dagger$ ). Signals at  $\delta$  124.9 to 138.5 in both spectra were assigned to vinylic carbon nuclei of the free zeaxanthin and the zeaxanthin moiety in the PEU. In the spectrum of PEU (Fig. 4b), the signals at 173.6 ppm, and 156.9 and 156.7 ppm correspond to ester and urethane carbonyl groups, respectively. The signal at  $\delta$  64.4 was assigned to the methylene bound to the  $sp^3$  oxygen of the ester group ( $-CO-O-CH_2-$ ). Further, the signal at  $\delta$  40.8 corresponds to the methylene bound to the urethane group ( $-CH_2-NH-CO-O-$ ), and the signal at  $\delta$  34.1 is ascribed to the methylene directly attached to the ester carbonyl group ( $-CH_2-CO-O-$ ). In addition, some signals corresponding to the carotenoid moiety, such as those of the methyl groups at  $\delta$  12.8 and 12.7, and that of the oxygenated methine at  $\delta$  65.0 (C-j) were identified. In the same manner, the  $^1\text{H}$  NMR spectrum confirmed the presence of the xanthophyll in the structure of the PEU (Fig. S13 $\dagger$ ).

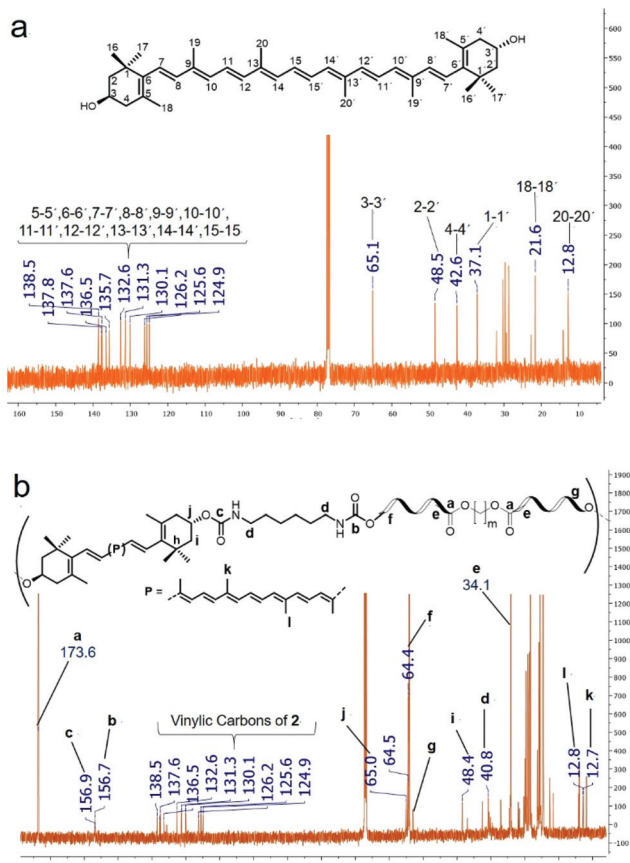


**Fig. 4** (a)  $^{13}\text{C}$  NMR spectrum of **2** in  $\text{CDCl}_3$  and (b)  $^{13}\text{C}$  NMR spectrum in  $\text{CDCl}_3$  of PEU derived from **2**

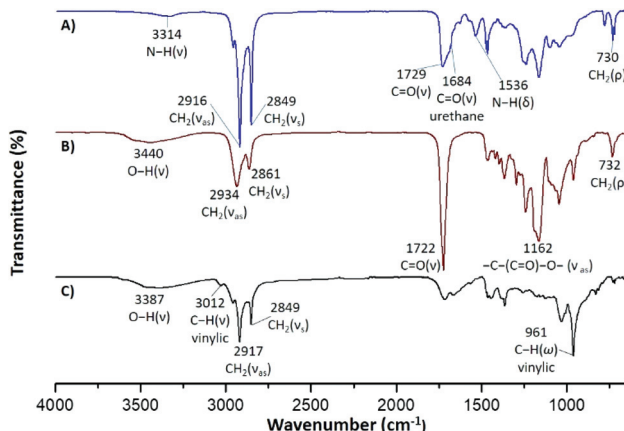


**Fig. 5** FTIR spectra of (A) PEUs synthesized from a macrodiol with DP = 5 and **1** as chain extender, (B) macrodiol with DP = 5, and (C) compound **1**.

Likewise, FT-IR analysis provided useful information for the characterization of the carbonyl groups present in the synthesized macrodiols and PEUs. The ester carbonyl at  $1729\text{ cm}^{-1}$  and the urethane carbonyl at  $1684\text{ cm}^{-1}$  were observed in the PEU film derived from **1** and the macrodiol with  $\text{DP} = 5$  [Fig. 5A]. Also, the bands at  $3314\text{ cm}^{-1}$  and

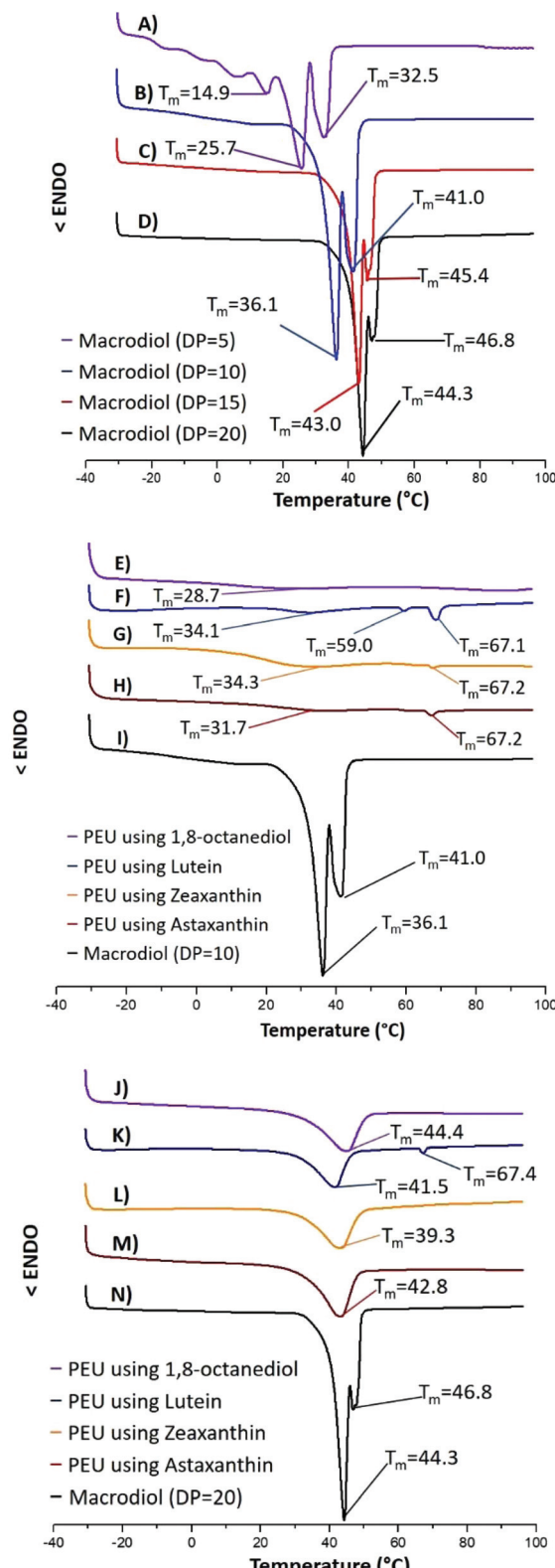


**Fig. 6** DSC thermograms of the four different macrodiols (A–D), the PEUs derived from the macrodiol (DP = 10) with the different chain extenders (E–I), and the PEUs derived from the macrodiol (DP = 20) with the different chain extenders (J–N). Conditions: 10 °C min<sup>–1</sup> (endo down); second heating cycle

1536 cm<sup>-1</sup> corroborated the N–H stretching and N–H scissoring modes of the urethane group, respectively. In the case of the poly( $\epsilon$ -caprolactone) diol (HOPCLOH) [Fig. 5B], a single band in the carbonyl stretching vibration region at 1722 cm<sup>-1</sup> accounted for the ester group  $[-(\text{C}=\text{O})-\text{O}-]$ . Regarding the xanthophyll 1 used as chain extender [Fig. 5C], a broad band at 3387 cm<sup>-1</sup> was attributed to the hydroxyl groups and another thin band at 3012 cm<sup>-1</sup> to the C–H stretching of the vinylic group.

Differential scanning calorimetry (DSC) was used to analyze this series of PEUs and their respective macrodiols. Fig. 6 shows the DSC thermograms of the four different macrodiols and those of a comparative series of PEUs derived from two macrodiols (DP = 10 & 20) and the different chain extenders (1, 2, 3, and Oct). The melting temperatures ( $T_m$ ) of the four HOPCLOHs were between 25.7 and 44.3 °C [Fig. 6A–D]. As can be seen, there is a clear increase in  $T_m$  as DP increases.

The melting points for the series of PEUs derived from the macrodiol with DP = 10, obtained in two steps with the different chain extenders, were observed between 28.7 and 34.3 °C (Fig. 5E–I) (Table 2). These results are very similar to those found for the series of PEUs derived from the macrodiol with DP = 10, which were obtained in a one-pot route (Fig. S18†). We did not observe a significant difference between the PEUs synthesized in two steps and those prepared *via* the one-pot route. The melting temperatures for the PEUs obtained using the three carotenoids as chain extenders were very similar (Fig. 5E–I).

The PEUs derived from Oct showed a lower  $T_m$  [Fig. 6E]. This series of PEUs (DP = 10) gave a similar second melting temperature ( $T_{m2}$ ) between 67.1 and 67.2 °C, which is attributed to the hard segment (HS) (Fig. 6F–H). To confirm this

assumption, the so-called hard segments were independently synthesized using HDI and one of the three xanthophylls. As expected, the resulting three polymers showed a unique  $T_m$  at 65 °C (Fig. S23†).

All PEUs showed similar behavior in their  $T_m$  values within each series, except those derived from the macrodiol with DP = 5, which had no crystallinity in its soft segment (Table 2) (Fig. S19†). No  $T_{m2}$  was observed in any of the PEUs derived from Oct, in contrast to those from lutein with a  $T_{m2}$  near to 67 °C. This characteristic could be attributed to the major asymmetry in 1, which has three stereocenters (3*R*,3'*R*,6*R*) compared with the meso-structures found in xanthophylls 2 and 3.

The melting points of the series of PEUs derived from the macrodiol with DP = 20 and the different chain-extenders were found between 39.3 and 44.4 °C (Fig. 6J–N). The  $T_m$  for the PEU prepared using Oct (Fig. 6J) was 44.4 °C, which is very similar to that of the macrodiol (44.3 °C) (Fig. 6N). The PEU prepared using 1 (Fig. 6K) had a melting point at 41.5 °C, and additional endothermic transitions were detected for this PEU at 67.4 °C, which were assigned to the hard segment melting temperature. On the other hand, the PEUs derived from the macrodiol with DP = 15 (Fig. S16†) showed similar  $T_m$  values to those of the PEU with DP = 20.

The effect of HOPCLOH on the crystallinity of the soft segment (SS) attributed to the PCL inside the PEUs was also studied. Fig. S24† shows the effects of the DP and the different chain extenders. All the PEUs showed a tendency towards increased crystallinity with increasing DP. Accordingly, the weight percent of the hard segment (wt% HS) had an important effect on the crystallinity of the PCL (Fig. S25†), thus,

**Table 2** Reaction conditions, thermal properties, and mechanical properties of the synthesized poly(ester-urethane)s (PEUs)

PEU: obtained with (DP)	$M_n$ HOPCLOH	Chain extender	HS (%)	Time <sup>a</sup> (Hours)	Soft segment		Hard segment		Stress at break (MPa)	Strain at break (%)	Modulus (MPa)
					$T_m$ (°C)	$\Delta H_m$ (J g <sup>-1</sup> )	$T_m$ (°C)	$\Delta H_m$ (J g <sup>-1</sup> )			
Oct(20)	2190	Oct	13.3	1.30	44.4	33.5	—	—	4.0 ± 0.9	2.9 ± 0.5	313.9 ± 23.8
1(20)	2190	1	20.4	2	41.5	29.2	67.4	0.5	3.6 ± 0.3	3.1 ± 0.4	284.5 ± 14.8
2(20)	2190	2	20.4	1.75	39.3	33.2	—	—	—	—	—
3(20)	2190	3	21.3	1.75	42.8	39.8	—	—	7.9 ± 0.2	22.8 ± 7.5	268.9 ± 7.9
Oct(15)	1670	Oct	16.7	1.25	43.4	22.7	—	—	3.4 ± 0.2	4.5 ± 1.1	180.6 ± 14.4
1(15)	1670	1	25.9	1.75	34.6	26.4	67.9	0.6	—	—	—
2(15)	1670	2	25.4	2	39.3	35.6	—	—	6.6 ± 0.2	16.9 ± 1.5	215.9 ± 7.2
3(15)	1670	3	25.8	2	36.8	31.1	—	—	6.1 ± 0.1	145.1 ± 56.6	133.0 ± 55.7
Oct(10)	1200	Oct	21.8	2	28.7	6.4	—	—	4.9 ± 0.4	59.8 ± 14.1	93.1 ± 6.5
1(10)	1200	1	31.6	5	34.1	4.6	67.1	4.4	4.9 ± 1.9	355.6 ± 155.8	37.2 ± 1.8
2(10)	1200	2	32.3	3.5	34.3	10.6	67.2	0.5	3.9 ± 0.4	355.1 ± 86.1	30.4 ± 3.4
3(10)	1200	3	34.3	1.50	31.7	3.7	67.2	1.0	2.2 ± 0.3	152.0 ± 14.2	6.1 ± 3.5
Oct(10) <sup>b</sup>	1200	Oct	22.9	1.75	23.9	4.4	—	—	—	—	—
1(10) <sup>b</sup>	1200	1	31.4	4	32.9	5.7	68.9	2.8	—	—	—
2(10) <sup>b</sup>	1200	2	31.8	3	26.8	8.5	67.5	0.2	—	—	—
3(10) <sup>b</sup>	1200	3	32.9	1.25	32.4	6.7	67.4	0.7	—	—	—
Oct(5)	645	Oct	34.9	1.25	—	—	—	—	12.7 ± 2.8	422.6 ± 106.7	199.4 ± 21.5
1(5)	645	1	46.1	1.75	—	—	67.0	5.5	4.6 ± 0.3	94.1 ± 11.5	93.6 ± 2.0
2(5)	645	2	46	2.50	—	—	66.8	2.8	3.0 ± 0.9	4.9 ± 1.2	155.6 ± 11.7
3(5)	645	3	46.5	1.50	—	—	—	—	6.9 ± 1.0	245.4 ± 71.6	51.7 ± 4.8

Oct = 1,8-octanediol; 1, 2, and 3 = xanthophylls. <sup>a</sup>Time of reaction. <sup>b</sup>Synthesized *via* a one-pot method.



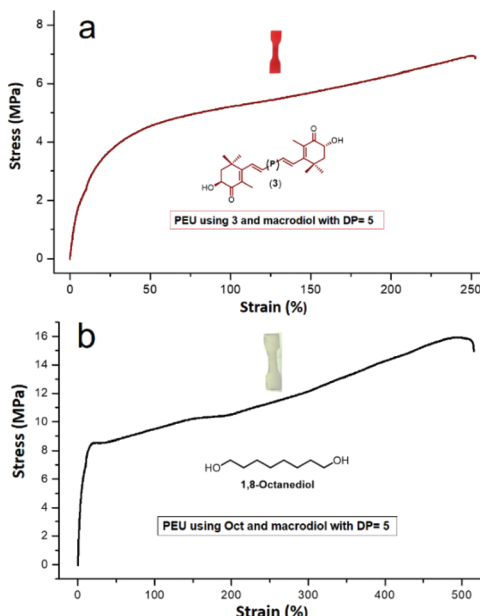


Fig. 7 Representative tensile data for PEUs derived from compound 3 (a) and those derived from 1,8-octanediol (Oct) (b).

when the HS was as high as 35% ( $\geq$ ) the SS did not show a melting transition and entered into an amorphous domain.

The mechanical properties of the PEU films were also tested. In Table 2, the low values of stress and strain at break and relatively high modulus values indicate plastic behavior of the PEUs. Comparing two different PEU samples derived from 3 and Oct (Fig. 7), both samples exhibited a plastic profile, where the incorporation of 3 in the main chain of the PEU induces low stress and strain at break and modulus with respect to the Oct sample. In this sense, in the majority of the PEU samples the values of modulus for species derived from Oct are higher than those of carotenoids (1, 2, and 3) (Table 2, Fig. S38†). This result suggests that the olefinic chain of carotenoids sterically hinders the intermolecular hydrogen bonding of the urethane groups. Additionally, the dependency of the crystallinity ( $\Delta H_m$ ) of the soft segment (PCL) on the modulus of the PEUs had a negligible effect (Fig. S40†).

Experiments to determine other properties and potential applications of the PEUs formed in this work are underway in our laboratory and eventually will be published in a future contribution.

## Conclusions

In summary, a new family of PEUs derived from carotenoids 1, 2, and 3 was successfully synthesized and characterized. The xanthophylls 1, 2, and 3 were found to be good chain-extender agents in the PEU synthesis and impart plastic behavior to their mechanical properties. It was shown that the carotenoids (1, 2, and 3) and hexamethylene diisocyanate (HDI) could generate their own microcrystalline domains, and some of the

PEUs exhibited double segregation of phases between the soft (PCL) and hard segments (1, 2, and 3/HDI), as detected by DSC. The xanthophylls 1, 2, and 3 represent an alternative use of natural products as precursors for PEUs with interesting structures and properties. More research into these novel PEUs is necessary to fully explore their potential uses as photoprotectors, and antioxidant materials that the intrinsic chemical properties of carotenoids may have given.

## Conflicts of interest

There are no conflicts to declare.

## Acknowledgements

E. R.-deL. thanks CONACYT for the doctoral fellowship and Fondo de Proyectos Especiales de Rectoría-UAQ under Grant number FOPER-2019-00967, for the financial support. E. R.-deL. and J. E. B. are highly thankful to Gerardo Fonseca-Hernandez, CFATA-UNAM for his technical support in evaluating mechanical properties, to Laboratorio Nacional de Caracterización de Propiedades Fisicoquímicas y Estructura Molecular, the University of Guanajuato for the NMR spectra recording, and Patricia Cerdá Hurtado (CIMAV-Unidad Monterrey) for the acquisition of the SEC chromatograms. J. E. B. thanks CONACYT Ciencia Básica for the grant "Proyecto SEP/284893" and DAIP CIIC 2019 (UG) "Proyecto 030/2019". J. E. B. thanks Kenneth J. Shea (University of California, Irvine) for his support in the acquisition of MALDI-TOF spectra.

## Notes and references

- 1 T. J. Lamdrum, *Carotenoids Physical, Chemical, and Biological Functions and Properties*, Taylor & Francis Group, Florida, 1st edn, 2001, pp. 3–4.
- 2 K. Jomova and M. Valko, *Eur. J. Med. Chem.*, 2013, **70**, 102–110.
- 3 R. Álvarez, B. Vaz, H. Gronemeyer and A. R. de Lera, *Chem. Rev.*, 2014, **114**, 1–125.
- 4 S. M. Rivera, *J. Nat. Prod.*, 2016, **79**, 1473–1484.
- 5 M. H. Walter and D. Strack, *Nat. Prod. Rep.*, 2011, **28**, 663–692.
- 6 G. Britton, S. Liaaen-Jensen and H. Pfander, *Carotenoids volume 5: Nutrition and Health*, Birkhäuser Verlag, Basel, 1st edn, 2009, pp. 7–8.
- 7 M. P. Horvath, E. George, Q. T. Tran, K. Baumgardner, G. Zharov, S. Lee, H. Sharifzadeh, T. Mattinson, B. Li and P. S. Bernstein, *Acta Crystallogr., Sect. F: Struct. Biol. Commun.*, 2016, **72**, 609–618.
- 8 A. Kijlstra, Y. Tian, E. R. Kelly and T. T. J. M. Berendschot, *Prog. Retinal Eye Res.*, 2012, **31**, 303–315.
- 9 A. Alves-Rodrígues and A. Shao, *Toxicol. Lett.*, 2004, **150**, 57–83.



- 10 D. A. Frey, E. W. Kataisto, J. L. Ekmanis, S. O'Malley and S. F. Lockwood, *Org. Process Res. Dev.*, 2004, **8**, 796–801.
- 11 R. Fassett and J. S. Coombes, *Molecules*, 2012, **17**, 2030–2048.
- 12 F. Visioli and C. Artaria, *Food Funct.*, 2017, **8**, 39–63.
- 13 J. E. Báez, A. Marcos-Fernández, A. Martínez-Richa and P. Galindo-Iranzo, *Polym.-Plast. Technol. Eng.*, 2017, **56**, 889–898.
- 14 J. E. Báez, D. Ramirez, J. L. Valentín and A. Marcos-Fernández, *Macromolecules*, 2012, **45**, 6966–6980.
- 15 H. Middleton, S. Tempelaar, D. M. Haddleton and A. Dove, *Polym. Chem.*, 2011, **2**, 595–600.
- 16 H. Tang, C. J. Murphy, B. Zhang, Y. Zheng, E. A. Vankirk and M. Radosz, *Biomaterials*, 2010, **31**, 7139–7149.
- 17 N. Shpaisman, N. Sheihet, J. Bushman, J. Winters and J. Khon, *Biomacromolecules*, 2012, **13**, 2279–2286.
- 18 S. Weintraub, T. Shpigel, L. G. Harris, R. Shuster, E. C. Lewis and D. Y. Lewitus, *Polym. Chem.*, 2017, **8**, 4182–4189.
- 19 This work is currently in progress and shows that the ROP of lactide using xanthophylls as initiators provides, through a similar process as the one described by Middleton and coworkers,<sup>15</sup> astaxanthin-containing poly(lactide)s.
- 20 E. Rodríguez-deLeón, J. E. Báez, J. O. C. Jímenez-Halla and M. M. Bah, *Molecules*, 2019, **24**(7), 1–13.
- 21 Sigma-Aldrich is now Merck, <https://www.sigmaaldrich.com/catalog/product/sial/phr1699?lang=en&region=GB>, (accessed November 2019).
- 22 J. E. Báez, A. Marcos-Fernández and A. Martínez-Richa, *Macromolecules*, 2005, **38**, 1599–1608.
- 23 J. E. Báez, M. Martínez-Rosales and A. Martínez-Richa, *Polymer*, 2003, **44**, 6767–6772.
- 24 J. E. Báez, A. Marcos-Fernández, R. Lebrón-Aguilar and A. Martínez-Richa, *Polymer*, 2006, **47**, 8420–8429.
- 25 L. Patiny and A. Borel, *J. Chem. Inf. Model.*, 2013, **53**, 1223–1228.

